Development of Novel Functional Conducting Elastomer Blends Containing Butyl Rubber and Low-Density Polyethylene for Current Switching, Temperature Sensor, and EMI Shielding Effectiveness Applications

Farid El-Tantawy

Department of Physics, Faculty of Science, Suez Canal University, Ismailia, Egypt

Received 19 March 2004; accepted 20 October 2004
DOI 10.1002/app.21778
Published online in Wiley InterScience (www.interscience.wiley.com).

ABSTRACT: A new class of functional conductive butyl rubber (IIR) with different loadings of low-density polyethylene (PE) was prepared by roll mixing in a milling at a rotor speed of 24 rpm. To understand the filler dispersion and filler/matrix interaction, the network structure of the specimens was examined by evaluating of the crosslinking density, volume fraction of elastomer, interparticle distance among conductive phases, interfacial area per unit volume, torque rheometer, hardness, tensile strength, elongation at break, X-ray, glass transition temperature, thermal gravemetry, differential scanning calorimetry, degree of crystallinity, and SEM microanalysis. Static conductivity, mobility carrier's concentration, number of charge carriers, and thermoelectric power as a function of PE content were investigated. The temperature dependence of the electrical conductivity as well as the conduction mechanism of IIR–PE blends were also analyzed. The isothermal resistance stability test was examined by displaying the resistance–time curve at certain temperatures. The relationship between current and DC applied voltage was measured for all samples. The self-electrical heater with PE content of 10 wt % exhibited the highest nonlinearity. The thermal stability was tested by means of temperature–time curve at certain applied power, on and off, for two cycles. Dielectric constant and relative loss factor of the blends are reported. The applicability of the rubber system for switching current, temperature sensor, and electromagnetic shielding effectiveness (EMI) was examined. The experimental results of EMI were compared with theoretical predictions. The results of the present study indicate that these blends are suitable for switching current, temperature-sensitive sensor, and EMI shielding effectiveness applications with good thermal stability for consumer products. © 2005 Wiley Periodicals, Inc. J Appl Polym Sci 97: 1125–1138, 2005

Key words: butyl rubber; low-density polyethylene blend; microstructure; current switching; temperature sensor; stability; electromagnetic interference shielding

INTRODUCTION

At present, there is a great interest in the design of new, addressable, functional conducting blends for use in various types of practical applications.[1,2] In fact, there are a number of problems involving the preparation of conducting blend such as weak interfacial adhesion, poor compatibility among two polymer phases, and high concentration of the conductive filler, which has to be considered and controlled to obtain a polymer blend with desirable properties. Mainly, two different approaches have been proposed to the solution of the above shortness in the blend. One is to use the organic and/or inorganic filler as an interfacial agent to the polymer system. The other is to introduce nonoscale filler as conducting charges.[3–7] Conductive filler can be incorporated as a second phase into these matrices to produce conductive polymer materials, which exhibit both percolation phenomenon and specific dependence of conductivity.[8–12] However, conducting polymer blends display, as some of their foremost properties, a high conductivity combined with very lightweight, flexibility, and easy processibility. Because of these properties and their high electrical conductivity/weight ratio, they have recently evinced much interest in potential applications. For a polymer-based negative temperature coefficient of conductivity (NTC) materials of practical value, the bulk conductivity decreases remarkably when temperature approaches the melting point of matrix resin.[13–15] Owing to the commercial significance of such a temperature-activated switch feature for electricity, a conductive polymer of this kind plays an increasing role in the polymer production community and serves as current switching, elements for suppression of in-rush current, relay delay, temperature control and sensing, fan control and self-electrical heaters, self resetting over-current protection elements, and microswitches.[16–21] Furthermore, all elec-

Correspondence to: F. El-Tantawy (faridtantawy@yahoo.com).

TABLE I
Different Loadings of PE in IIR Blends[a]

Ingredients (phr)	PE0	PE10	PE20	PE30	PE40
IIR	100	90	80	70	60
PE	0	10	20	30	40
ZnO	5	5	5	5	5
Stearic acid	2	2	2	2	2
Glycerol	10	10	10	10	10
CB	25	25	25	25	25
TMTD[b]	1	1	1	1	1
CBS[c]	1	1	1	1	1
Sulfur	2	2	2	2	2

[a] The ingredients are arranged in the same order used during preparation.
[b] Tetra methyl thiuram disulfide.
[c] *N*-cyclohexylbenzethiozole sulphenamide.

trical and electronic devices emit electromagnetic signals. Electromagnetic interference shielding effectiveness (EMI) is now mandatory by government agencies worldwide for shielding of most devices.[22] Therefore, conducting polymers with relatively high electrical conductivity and dielectric constant are promising materials for EMI shielding applications, such as EMI screens, static charge dissipation, coatings or jackets for flexible conductors, and broadband microwave absorbers. With the above light, in this article, a new type of conducting elastomer blends based on butyl rubber (IIR) and low-density polyethylene (PE) was developed. The effect of PE loading on the change of the network structure was investigated in detail. Also, the effect of PE content on the electrical conductivity, and dielectric constant was analyzed. The applicability of the proposed blends for switching current, temperature sensor, and EMI will be reported. The thermal stability of IIR blend was tested by means of isothermal resistance versus time and applied power on and off for several cycles.

EXPERIMENTAL

Butyl rubber, low-density polyethylene, and the other compounding ingredients in Table I used for preparing the blends were supplied by Kuko Du Chemical Industry Co., Ltd. (South Korea). The formulations of the blends are shown in Table I. The blends were prepared on a conventional laboratory-size rubber mill with 170 mm diameter, working distance of 300 mm, speed of slow roll of 24 revolutions/min, and gear ratio of 1.4. The compounded rubber was left for at least 24 h before vulcanization. Crosslinked samples of desired thickness were produced by compression molding at 155°C and a pressure of 250 KN/m^2 for 30 min in an electrically heated press. The furnace carbon black (CB) with a commercial name of porous black was supplied by Asahi Carbon Co. Ltd. (Niigata, Japan) with a particle size of 1 μm and a surface area of 290 m^{2}g^{-1}, used as a conductive filler component in the blend. The cure characteristic was studied in a Mansanto rheometer at 155°C. The morphology of the polymer samples was examined by scanning electron microscope (SEM, JSM-5210, LVB, Jeol). Surface tension (S_E) was measured by using a surface tensionmeter model GPA-A4 (Tokyo, Japan). The densities of polymer specimens were measured by Archimedes method. The densities of green specimens were obtained by measuring the masses and the dimensions of the samples.[1] The crosslink density (CLD) of the IIR–PE blends was determined on the basis of rapid solvent-swelling measurements (toluene for 24 h at 20°C) by application of[15,23]

$$-\ln(1 - V_r) - V_r - \chi V_r^2 = \frac{V_0}{\mathrm{CLD}}\left(V_r^{(1/3)} - \frac{V_r}{2}\right) \quad (1)$$

where V_r is the volume fraction of the IIR in the swollen mass, V_0 is the molar volume of the solvent, and χ is the interaction coefficient between rubber network and solvent, which could be calculated by

$$\chi = (\delta_s - \delta_r)\frac{V_0}{RT} \quad (2)$$

where δ_s and δ_r are the solubility parameters of the solvent and the rubber network, respectively, R is the universal gas constant, T is the absolute temperature, and V_r is calculated by the expression

$$V_r = \frac{m_0\phi(1 - \alpha)\rho_r^{-1}}{[m_0\phi(1 - \alpha)\rho_r^{-1} + (m_1 + m_2)\rho_s^{-1}]} \quad (3)$$

where m_0, m_1, and m_2 were the weights of the rubber samples in air, swollen state, and after drying in a vacuum oven at 60°C for 24 h, respectively, ϕ was the mass fraction of rubber in the vulcanizate, α was the mass loss of the IIR vulcanizate during swelling, and ρ_r and ρ_s were the rubber and the solvent density, respectively.

The interparticle distance (IPD) among conductive phases is calculated by[1,24]

$$\mathrm{IPD} = d\left[\left(\frac{k\pi}{6V_r}\right)^{1/3} - 1\right] \quad (4)$$

where d is the CB particle diameter and $k = 1$ for cubic packing.

The interfacial area per unit volume of the blend was calculated using the equation[3]

$$A = n \times 4\pi(R_c^2 + R_h^2) \quad (5)$$

where A is the total area occupied by the dispersed phase (i.e., CB and PE), R_c and R_h are the radius particles of CB and PE, respectively, and n is the number of particles per unit volume in the rubber system, which can be estimated from[5,25]

$$n = \frac{\theta_c + \theta_h}{4/3\pi(R_c^3 + R_h^3)} \quad (6)$$

where θ_c and θ_h are the volume fractions of CB and PE, respectively.

X-ray diffracting (XRD) patterns of the conducting rubber system were recorded on a Regako X-ray diffractometer by using CuKα radiation at 30 kV and 150 mA. Thermal analysis was performed by using a Seiko DSC 15200 instrument system, consisting of thermogravimetric analysis, differential thermal analysis (TG/DTA 220), and differential scanning calorimetry (DSC) 220 instruments. Thermal experiments were carried out with a heating rate 5°C/min in air atmosphere. The degree of the crystallinity (D_c) was determined by using the equation[2]

$$D_c = \Delta H_f/(\Delta H_f^0 W_f) \quad (7)$$

where ΔH_f is the apparent enthalpy (indicated in DSC thermograms as melting enthalpy per gram of rubber system) of fusion corresponding to the component, ΔH_f^0 is the enthalpy of fusion per gram of the component in its completely crystalline state, and W_f is the weight fraction of the component. The volume conductivity temperature dependence was performed on cured samples by DC two-probe method by using a computer-aided system in the temperature range of room temperature to 200°C in air. To ensure a good contact, the two ends of the rubber specimens were covered with brass cupper sheet during the vulcanization process.[1] The isothermal stability tests were carried out by incubation of the rubber samples in an electric oven held at 115°C. The resistance as a function of time was monitored in the samples by using a Keithly electrometer type 442. The thermoelectric power (TEP) measurements were made by gripping the samples between two blocks of silver. Two copper constantan thermocouples were embedded 2 cm apart on the samples to measure the temperature gradient across these samples (ΔT) produced by a small commercial heater attached to one of the silver blocks. The Seebeck voltages (ΔV) were measured through the silver leads in air according to the formula

$$\mathrm{TEP} = \frac{\Delta V}{\Delta T} \quad (8)$$

The dielectric constant was estimated via a Hewlett–Packard impedance analyzer. The mechanical properties of different PE-filled vulcanizates were determined by using a universal testing machine. The hardness of the blends was measured by using a Durometer, shore A (ASTM D2240-87). The Hewlett–Packard waveguide line containing spectroanalyzer, power matter, coefficient of reflection meter, and coefficient of attenuation meter determined the electromagnetic interference shielding properties. The measurements were carried out in the frequency ranges of 1 to 15 GHz.

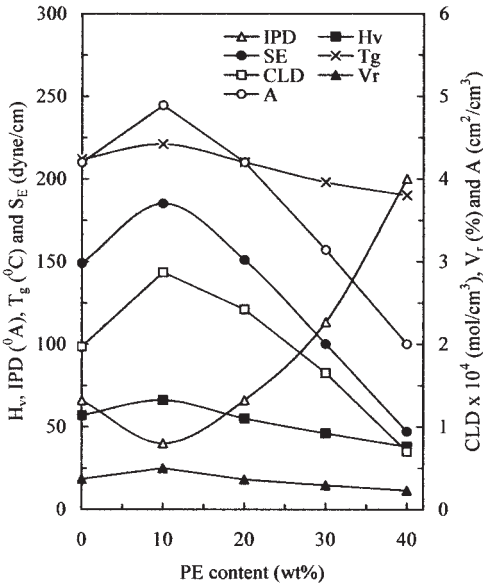

Figure 1 Crosslinking density (CLD), volume fraction of elastomer (V_r), average inter particles distance among conductive phases (IPD), interfacial area per unit volume (A), surface tension (S_E), glass transition temperature (T_g), and hardness (H_A).

RESULTS AND DISCUSSION

Effect of PE content on the network structure of the blends

To study the effect of PE content in more detail and its potential effect on network structure of the IIR composite, CLD, volume fraction of elastomer (V_r), average interparticle distance among conductive phases (IPD), interfacial area per unit volume (A), and hardness (H_v) were estimated, as demonstrated in Figure 1. It can be observed that, as the PE content increases up to 10 wt %, the CLD, V_r, and H_v increases, whereas the IPD decreases. On the contrary, by increasing PE more than 10 wt %, the CLD, V_r, and H_A decreases, whereas IPD increases. Higher CLD, V_r, and H_v are observed by increasing the fraction of PE up to 10 wt %. One plausible explanation for the increase of the CLD can be ascribed to the facile mobility carriers and the polymer–polymer interaction, which induces the rigidity of the polymer chains.[3–6] Also, it is worth noting that the PE10 sample gave a higher hardness compared

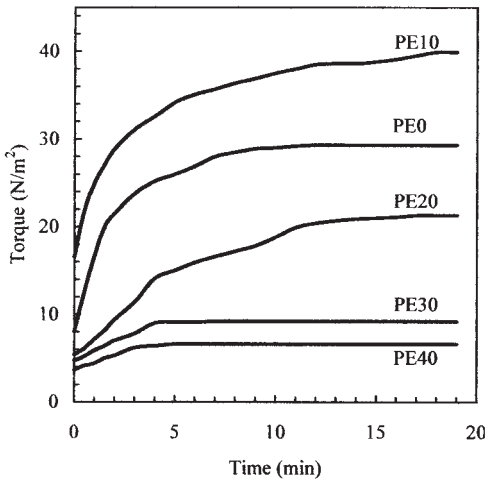

Figure 2 Torque rheometry for IIR/PE blends.

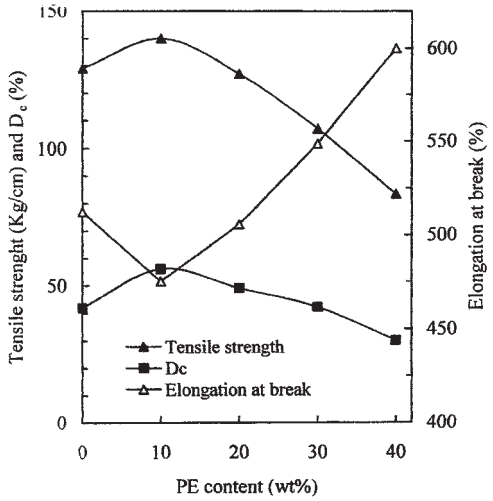

Figure 3 Tensile strength, elongation at break, and degree of crystallinity (D_c) as a function of PE contents for IIR/PE blends.

with other samples, which indicates that there is some sort of interaction between polymer and filler. The highest hardness of PE10 sample is ascribed to the complete compatibility with IIR matrix and the polymer blend molecules are very compact. The IPD of the disperse phases for PE10 sample was smaller than those in others. Thus, the incorporation of PE less than 20 wt % to IIR matrix improves its compatibility and connectivity among conductive phases. This makes the dispersion of PE in IIR matrix better and works as a compatibilizer agent to give a polymer blend. This reflects the chain connectivity and interfacial adhesion increases in the blends with increasing PE content up to 10 wt %, as confirmed above. For further confirmation of the above facts, interchain crosslinking reaction is studied by torque rheometry as shown in Figure 2. Torque is found to increase in the case of the PE10 sample compared to others. Increment of torque in PE10 is due to the formation on interchain crosslinking and higher friction between PE and IIR matrix. In other words, the rate of crosslinking increases with increasing volume fraction of PE in the blend up to 10 wt %. On the other hand, samples PE30 and PE40 do not undergo interchain crosslinking reaction, as its torque value remains constant. We believe that, at low content of PE less than 20 wt %, the liquid phase forming during curing process results in better quality of the network structure and adhesion at the interface boundary into matrix resin. This argument is also confirmed by measured the surface tension (S_E) and glass transition temperature (T_g) of the blend as a function of PE content, as shown in Figure 1. The increase of S_E and T_g for sample PE10 is a strong clue that the PE, up to 10 wt %, enhances the interfacial adhesion (i.e., crosslinking efficiency) and restricts the polymer chain mobility; therefore, the rigidity of chains increases into the blend system. To clarify this effect, measurements of tensile strength and elongation at break as a function of PE contents were performed, as shown in Figure 3. The tensile strength of the sample increases up to 10 wt % and then decreases with increasing PE content in the blend. This behavior may be explained by the fact that the segregation along the polymer–filler interface is due to the weak adhesion between filler and matrix when increasing PE content more than 10 wt %. In addition, when PE $>$ 10 wt % was added, the intermolecular forces within rubber matrix decrease led to more flaws in the rubber matrix and lower crosslinking density, as confirmed by CLD in Figure 1. The tensile strength increased at a maximum value at 10 wt % PE and then decreased. This can be explained by the increase of the degree of crystallinity (D_C) of the rubber matrix caused by the addition of PE up to 10 wt % in Figure 3.

Figure 4 shows the XRD patterns of the rubber

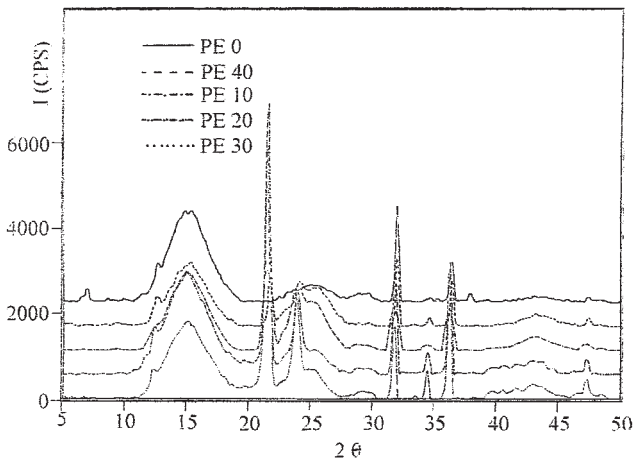

Figure 4 XRD patterns of the rubber for IIR blends.

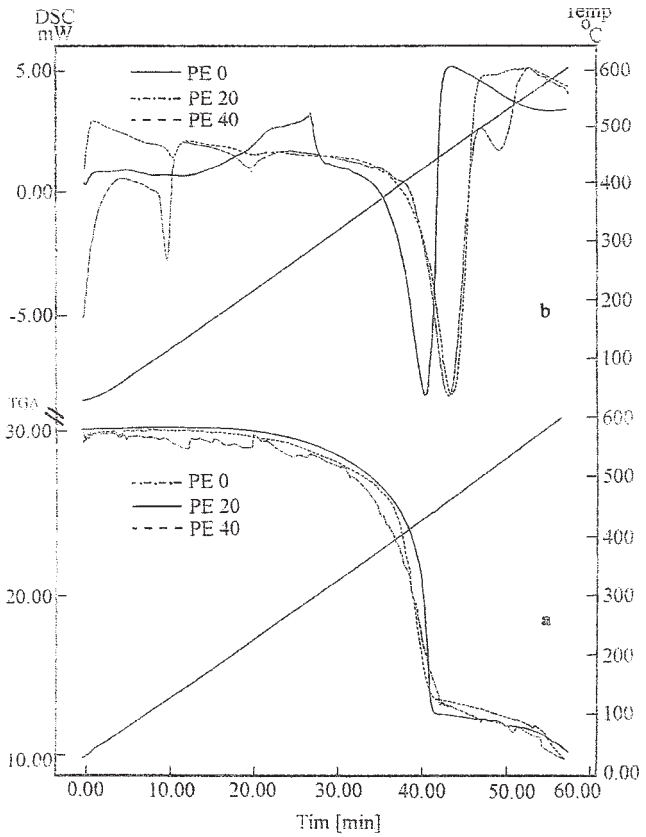

Figure 5 (a) TGA curves for IIR–PE blends. (b) DSC curves for IIR–PE blends.

blend. The crystalline peaks at 25.0°, 33.4° refers to the IIR rubber; crystalline peaks at 10.9° and 19.5° refer to CB, and crystalline peaks at 21.5°, 24.2°, and 34.5° refer to PE. It is observed that the addition of PE had a significant effect on the crystallinity of IIR matrix. The crystallinity of the rubber matrix increased a lot when 10 wt % PE was added and then decreased by increasing more PE into the rubber matrix. The rubber charged with PE powder has a higher thermal stability than the uncharged rubber. This assertion is based on the analysis of the TGA curves plotted in Figure 5(a), which shows that the temperature at thermal decomposition of the composites shifts to higher temperature with the increase of PE content up to 10 wt % compared with other samples. The slight increase in the decomposition temperature with the increase of PE content in the blend may be explained by the increase of its degree of crystallinity as supported by the result obtained from XRD and DSC results. Figure 5(b) depicts typical DSC scans of the rubber and its blends for samples PE0, PE10, and PE40. The endothermic peak for the PE0 sample is associated with the melting of crystals composed of an isobutylene/isoprene sequence on the IIR chains.[7–10] Also, it is observed that the melting temperature has been slightly shifted to a higher temperature and a new exothermic peak appears for PE10 and PE40 samples. This may be attributed to the improvement in the crystal perfection of polymer matrix.[11,12]

Surface morphology of the blends

Figure 6(a–c) shows the SEM micrograph of IIR system for samples PE0, PE10, and PE40, respectively. It can be seen that there are remarkable differences between unfilled and filled IIR composites as to grain distribution. For unfilled PE (i.e., sample PE0), the CB is completely fragmented, resulting in better homogeneity and distribution into rubber matrix. The shapes of most grains are approximately globular and/or round. On the other hand, the grains of conductive IIR filled with PE have distribution of PE fiber with various shapes and orientation into the matrix. Sample PE10, the PE forming fiberlike and good interface adhesion with IIR matrix, has an advantage in forming the conducting network (i.e., high aspect ratio) into polymer matrix. With increasing PE content more than 20 wt % (i.e., sample PE40), the density of PE fiber increases and harms the chain connectivity into IIR matrix. This factor together with the poor adhesion of PE to the IIR matrix is responsible for the deterioration of electrical and EMI shielding properties with increasing PE concentration, as evidenced later in this article.

Percolation behavior, mobility carriers, and thermoelectric power

The percolation threshold of the electrical conductivity (σ) depends very much on the geometry of conductive filler, interface adhesion, and polarity of the blend. Thereby, the concept of percolation can be used to understand the change in σ as a function of filler concentration in metal–insulator blends. Variations of the σ, mobility carriers (μ), and TEP of the rubber system with respect to PE content are displayed in Figure 7. It is very clear that the maximum value of σ is observed at 10 wt % PE. An addition of PE $<$20 wt % shows improvement in the σ and μ in the blends. One important point noticed is that both σ and μ increase with increasing PE content up to 10 wt % and then decrease. The first reason for the increase of the σ and μ for sample PE10 is the possibility of a manifestation of the increasing ramification of conducting network (i.e., build infinite cluster) over the entire blend.[13–16] The second reason is the lower contact resistance of conductive paths caused by the reduction of the interface free energy that helped to increase the maximum blend conductivity, as evidenced before by S_E results. The decrease in σ with increasing PE content more than 20 wt % may be due to partial blockage of conductive path by the PE molecules embedded in the IIR matrix, as confirmed by SEM photographs in

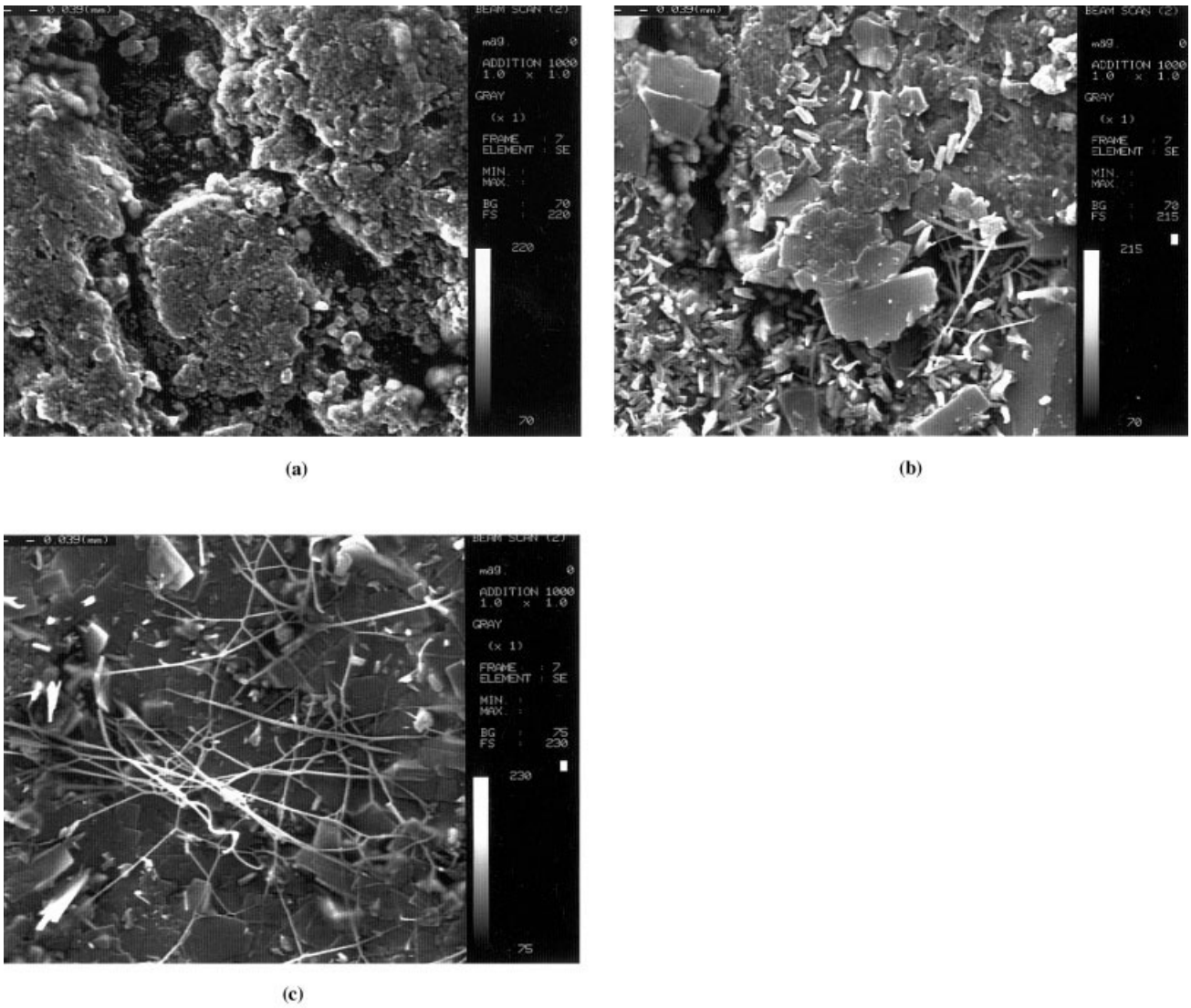

Figure 6 SEM micrograph of IIR blend for samples PE0, PE10, and PE40, respectively.

Figure 6(b). Thus, it can lead to the conclusion that the motion of charge carriers in the matrix is restricted by the PE fiber at high concentrations more than 10 wt % (i.e., PE20, PE30, and PE40 samples). Based on the above arguments, it may be postulated that PE lower than 20 wt % plays the role of an interphase builder (i.e., compatibilizer). In Figure 7, the variation of TEP as a function of PE content is found to be negative over the entire range of concentration studied. Thereby, it can be concluded that the IIR blend is an *n*-type semiconductor and the majority charge carriers are electrons.[23,24]

Conductivity-temperature characteristics

The results of earlier studies of IIR–PE blends always showed a linear decrease of conductivity with temperature for PE0, PE10, and PE20 samples, exhibiting a

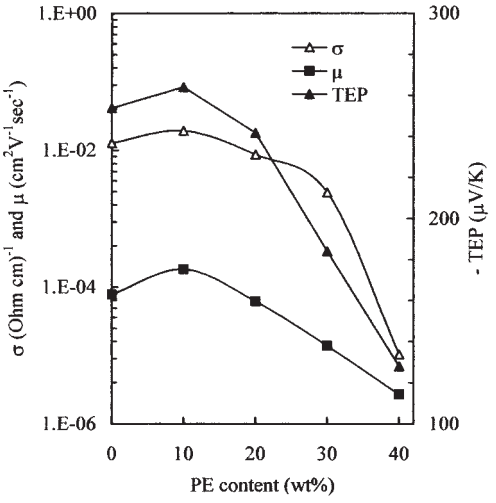

Figure 7 Variations of the σ, mobility carriers' (μ), and thermoelectric power (TEP) of the rubber system with respect to PE content.

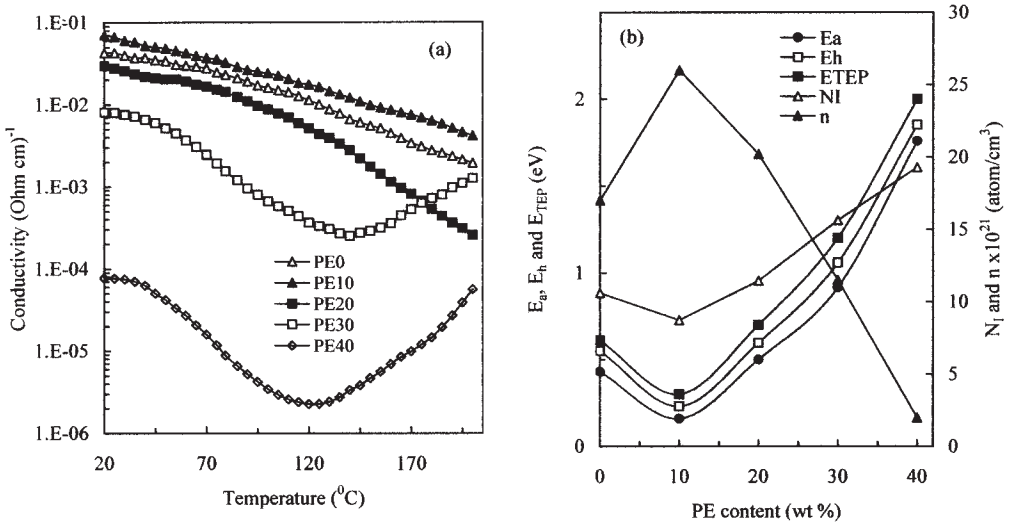

Figure 8 (a) Conductivity–temperature curves of conductive IIR blends with different contents of PE. (b) Activation and hopping energies (E_a), (E_h), E_{TEP}, n, and N_I of IIR blend as a function of PE content.

semiconductor behavior. The blends showed a V-shaped conductivity temperature characteristic (i.e., negative and positive temperature coefficient of conductivity NTC/PTC) for PE30 and PE40 samples in Figure 8(a). The decrease of conductivity with temperature is due to the disturbance in the continuity of the conducting paths caused by the thermal expansion of rubber matrix.[24,25] With relatively high temperature, the conductivity rapidly decreases. This may be attributed to a deagglomeration of conductive paths principally caused by the bulk expansion of the matrix, which breaks the conducting networks. Another possible explanation of the decrease of the conductivity with temperature is related to the rapid increase of interparticle distance between conductive paths, caused by the rapid expansion from crystalline to amorphous.[17,19] Since the density of the amorphous zone is lower than that of the crystalline zone, it is generally believed that the increase of long spacing is responsible for lamellar size. The larger the lamellar size is, the greater the volume fraction of amorphous zone resulting from crystalline melting becomes, and the larger the widening between conductive paths dispersed in an amorphous zone is pulled, the lower the conductivity, therefore, decreases. The slow rise in conductivity after switching temperature for samples PE30 and PE40 is attributed to the thermal expansion in the amorphous region, while the thermal expansion in the crystalline region is negligible. When partial melting takes place at higher temperature (i.e., after switching temperature), the conductivity begins to increase and the marked transition of a positive temperature coefficient of conductivity (PTC) curve begins to emerge. A feature of interest in this figure is that, for PE30 and PE40 samples, an abrupt conductivity transition occurs at a creation temperature, which can be designated as the new double-negative/positive temperature coefficient (NTC/PTC) thermistors. We believe that at the switching temperature the polymer chains and/or segments have sufficient mobility carriers. Therefore, the PTC phenomena can be accounted for by the formation of conductive phases resulting from the relaxation of blend structure and the agglomeration of conductive particles. However, the NTC intensity (N_I) is calculated according to

$$N_I = \log(\rho_{\max}/\rho_{RT}) \tag{9}$$

where $\rho_{\max}$ is the maximum resistivity value, and ρ_{RT} is the resistivity at room temperature.

The estimated values of N_I as a function of PE content are plotted in Figure 8(b). It is observed that the N_I intensity first decreases with the increasing PE content up to 10 wt % and then increases after the volume fraction reaches 20 wt %. In other words, the addition of PE up to 10 wt % enhanced the thermal stability of polymer matrix as confirmed before by TGA and DSC results.

Conduction mechanism of conductivity

The σ-T curve shows that the conduction mechanism is mainly thermally activated according to the known relationship

$$\sigma = \sigma_0 \exp(-E_a/KT) \tag{10}$$

where σ_0 is the temperature-independent parameter, K is the Boltzmann's constant, and E_a is the apparent activation energy.

Also, the hopping energy (E_h) can be calculated as

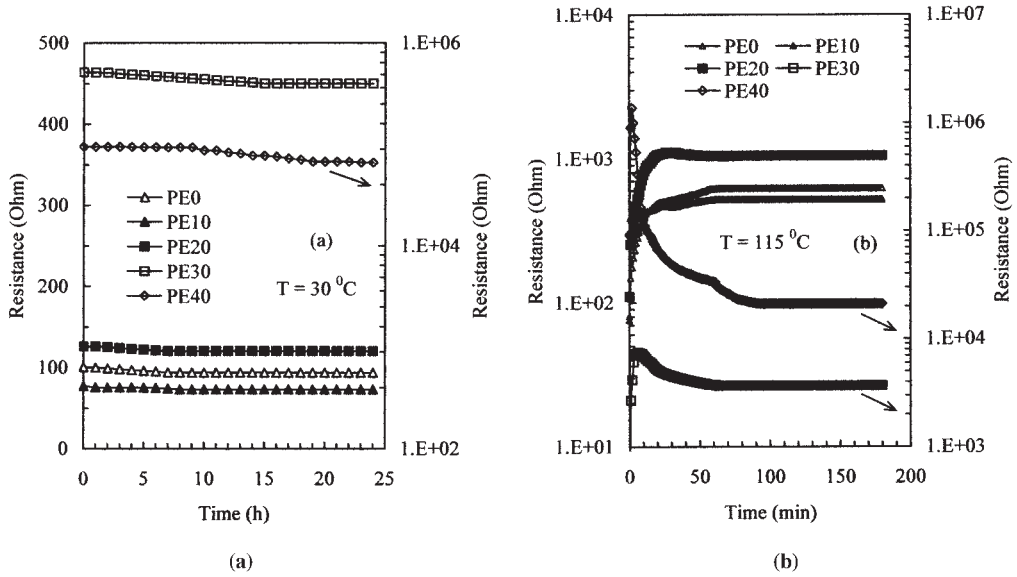

Figure 9 (a) Variation of resistance of the IIR–PE blend as a function of the aging time at temperature 30°C. (b) Variation of resistance of the IIR–PE blend as a function of the aging time at temperature 110°C.

$$\sigma \sqrt{T} = \sigma_0 \exp(-E_h/KT) \tag{11}$$

Figure 8(b) shows the activation and hopping energies (E_a) and (E_h), respectively, of IIR blend as a function of PE content. It is obvious that the value of the E_a and E_h is reduced for samples PE0 and PE10. By increasing PE content more than 10 wt %, the E_a and E_h were increased. The lower activation energy obtained in the PE10 sample is possibly derived from the high mobility carrier's homogeneity and interface adhesion of the IIR–PE blend. It is interesting to observe that the calculated values of E_a and E_h are very close. This reflects that the conduction mechanism of IIR blends is controlled by hopping mechanism.[20] As more confirmation, we calculated the values of activation energy from thermoelectric power (E_{TEP}) by using

$$\text{TEP} = \pm \frac{K}{e}\left(\frac{E_{\text{TEP}}}{KT} + F\right) \tag{12}$$

where e is the elementary charge and F is a constant in between 2 and 4.

The estimated values of E_{TEP} as a function of PE content are plotted in Figure 8(b). The higher value of E_{TEP} (in comparison with E_a) can be connected to the fact that the n-type conduction mechanism as confirmed by TEP results before. Based on the above facts, we speculate that, in the case of PE0, the Fermi level is above the middle of the gap (i.e., n-type conduction). Increasing PE content up to 10 wt % leads to the shift of the Fermi level to slightly above the middle of the gap and the conductivity increases. The effect of electrons on conductivity will increase the concentration of current carriers. We suppose that the addition of PE into rubber system leads to a redistribution and appearance of new defect states in the gap (i.e., pinning states). The influence of donorlike state slightly increases and also the mobility of electrons increases. Increasing PE more than 10 wt %, the Fermi level shifts close to the middle of the gap and the conductivity decreases (i.e., resistivity increases). This is why the conductivity increases with increasing PE volume fraction up to 10 wt % and then decreases when PE content exceeds 10 wt % into the matrix, as observed before in Figure 7.

Isothermal resistance stability test

In fact, the problems of reliability lifetime of thermistors and resistance to the attacks by heat and aging time are very important from a scientific and practical viewpoint. Figure 9(a) gives the variation of resistance of the IIR–PE blend as a function of the aging time at a temperature of 30°C. The resistance of the samples slightly decreases at the beginning of 5 h and then steadies up to 24 h, depends on PE content. This is due to the fact that the crosslink density in the interface of the IIR–PE vulcanizate by thermal aging increases. Furthermore, the diffusion of conductive particles and chain segments agitates more violently within the polymer matrix. The resistance against time at certain temperatures of about 115°C of the blends is shown in Figure 9(b). It is clear from the figure that the resistance increases suddenly and after certain time levels off, depending on PE content. The sudden increase of the resistance is mainly due to the volumetric thermal expansion of the blend and increases the thermal driving force for conductive particles to agglomeration.[21]

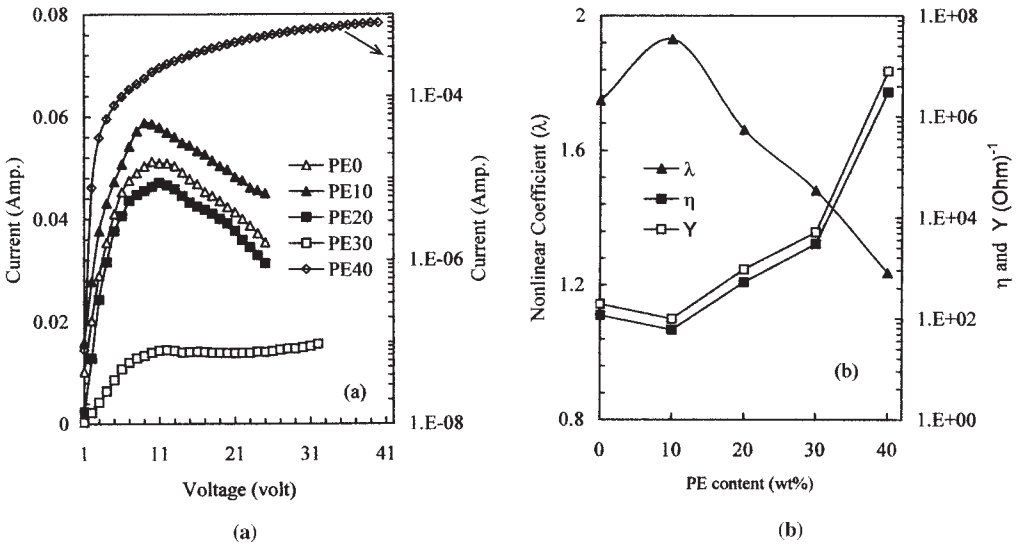

Figure 10 (a) The *I–V* curves of conductive IIR–PE blends and (b) Parameter k and α calculated based on the data in (a) and according to equation 10, and measured conductance (Y) independence on PE content.

Applicability of blends in switching current

The current–voltage (*I–V*) curves of conductive IIR–PE blends are presented in Figure 10(a). It is obvious that the *I–V* characteristic is similar to that of conventional NTC thermistors.[1–4] There is remarkable deviation from the Ohmic relation in the *I–V* curve. There is no Joule heating observed in the non-Ohmic regions. At low PE content (i.e., sample PE10), the specimens are more conductive; therefore, larger current can flow through at low applied voltage. The bulk temperature of the specimen increases with increasing applied potential. The heat dissipation is high at large potential, which may induce high Joule heating and the possible nonlinear behavior. It seems that the nonlinear conduction starts at lower potential and the current in the non-Ohmic zone is very high. This implies that the proposed blend is useful for low-voltage power regulation systems, such as battery-operated motors, spark quenching, and low-voltage electronic switches. However, the nonlinear conduction is due to the carrier's transport across the grain boundaries by means of inelastic tunneling through pinning centers of the blends and/or the decrease of the insulating barrier's height in the grain boundary zone in the blend. On the other hand and with respect to samples PE30 and PE40, the nonlinear behavior is controlled by the existence of double Schottky potential at the grain boundaries. Finally, it is important to mention that, in the samples PE30 and PE40, no switching effect is observed.

However, the *I–V* relation in Figure 10(a) can be described by[18]

$$I = \eta V^{\lambda} \tag{13}$$

where η and λ are empirical constants, independent of the applied potential. η is the conductance and λ is the deviation from Ohmic (linear) law. $\lambda = 1$ indicates Ohmic contact between the conductive paths. Non-Ohmic behavior $\lambda \neq 1$ is often reported for conductive polymer of second conductivity mechanism caused by the presence of dielectric zones in the path of the charge carriers.[25]

η and λ fitted with respect to the data in Figure 10(a) are reported in Figure 10(b) as a function of PE content. This result indicates a typical nonlinear behavior for IIE–PE blends. The conductance (Y) measured before the filled applying agrees well with η in Figure 10(b).

Applicability of blends in temperature sensor

Figure 11 shows the variation of the temperature with applied voltage of IIR–PE blend. These materials showed a gradual increase in temperature with applied electric field. Also, from these curves, one may easily observe that the increase of PE more than 10 wt % in the blends induces a decrease of their ultimate surface temperature. Moreover, the maximum temperature value of the PE10 sample is much higher relative to the other samples. For PE0, PE10, and PE20 samples, the temperature increases linearly with increasing applied voltage. It was suggested that the presence of PE less than 20 wt % improved the molecular structure of the blends. Hence, we recommended materials (i.e., PE0, PE10, PE20, and PE30 samples) as temperature sensors for commercial application.

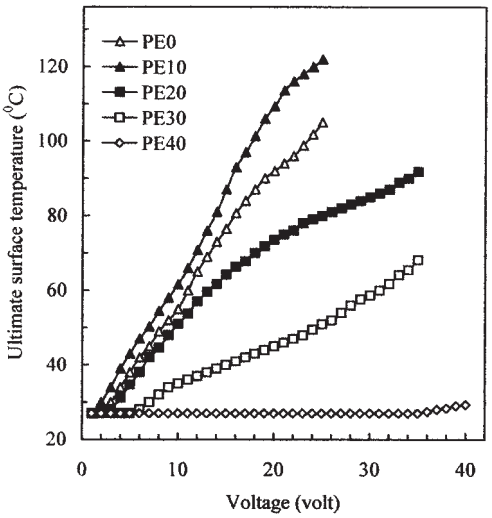

Figure 11 Variation of the temperature with applied voltage of IIR–PE blend.

Current–time (*i–t*) curve

Again, to evaluate the stability of the samples under potential operation, the current dependence of the time for the sample under a constant applied potential of about 25 *v* was measured. The *I–t* behavior of the IIR system is plotted in Figure 12(a). From the decay current records of Figure 12(a), it can be seen that the maximum current for the sample PE10 increases compared with PE0, PE20, PE30, and PE40, respectively. This result could be explained by the bulk charge of the blends (i.e., increase of interfacial adhesion and crosslinking density), leading to an increase of maximum current. Thus, it can be said that the incorporation of PE up to 10 wt % to IIR rubber improves its compatibility. For the PE40 sample, current is almost a constant, whereas for PE0, PE10, and PE20 samples, current decreases with time, due to the voltage-controlled positive resistance effect. This electrical self-heating effect leads finally to an electric-thermal equilibrium current, I_c. The higher the PE content, the higher the resistance, and thus, the lower the mobility carriers (i.e., current) because the self-heating effect is almost eliminated by the higher resistance and the lower time dependence of the current.

However, the *I–t* curve may be described by the discharge exponential equation as

$$\frac{I_t - I_0}{I_m - I_0} = \exp(-t/\tau_d) \tag{14}$$

where I_t is the current at a given time (t), I_0 is the current at time zero, I_m is the maximum current when applied voltage level on, and τ_d is the characteristic decay time constant.

The physical meaning of this parameter gives us information about the macroscopic stability of current with time, information needed for self-heating applications. Therefore, the estimated values of τ_d as a function of PE content are given in Figure 12(b). It is observed that τ_d decreases up to 10 wt % PE and then increases with increasing PE more than 10 wt %. This implies that the inclusion of PE up to 10 wt % enhanced the thermodynamically stability into rubber matrix. From Figure 12(a), the transport numbers corresponding to electronic conduction (T_{nec}) were calculated by using[25]

$$T_{nec} = \frac{I_c}{I_i} \tag{15}$$

where I_i and I_c are the initial and steady-state current, respectively.

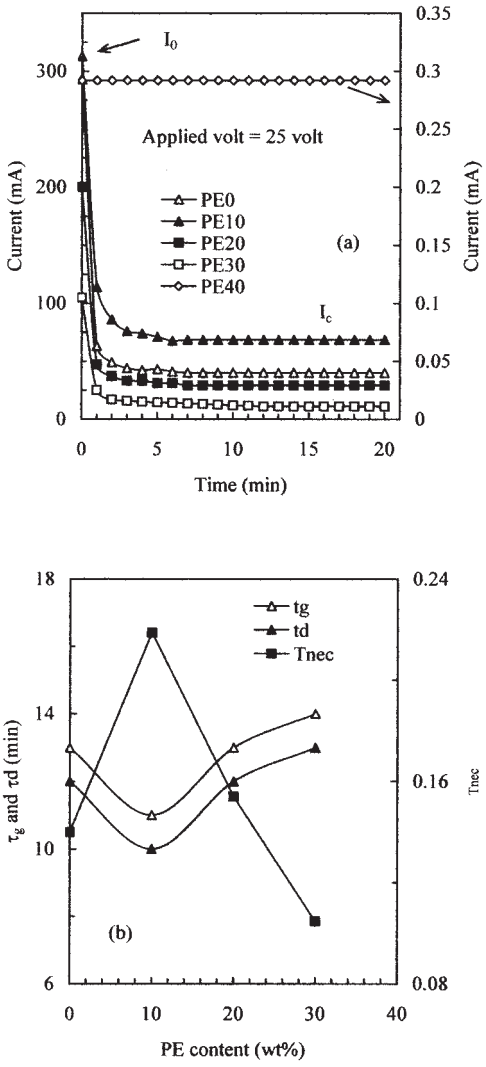

Figure 12 (a) The *I–t* behavior of IIR system under certain applied voltage and (b) the estimated values of τ_d and τ_g as a function of PE volume fraction of IIR blend.

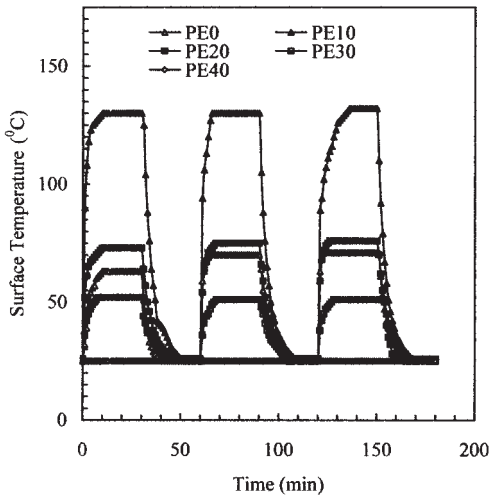

Figure 13 Temperature against time under applied certain power is about 0.4 W on and off for three cycles of IIR blends.

The estimated transport number as a function of PE content is recorded in Figure 12(b). This value suggests that the charge carriers in the IIR–PE blend is predominantly due to electronic, as confirmed by TEP data before.

Stability test under applied certain power

Important for all applications specifically in electrically self-heating is the thermal stability of the blend under applied potential. Thus, we focus on understanding the thermal stability of IIR–PE blend by continuously displaying the temperature of the specimens over time at certain applied powers is about 0.4 W on and off for three cycles. Figure 13 shows the temperature against time under applied voltage on and off for three cycles of IIR blends. Curves in Figure 13 show very similar growth of temperature in the beginning of applied voltage and after a certain time levels off. It is clear that the sample PE10 shows a higher temperature compared to other samples at the same applied voltage. This clue suggests that, with the addition of PE less than 20 wt %, the rubber matrix is thermodynamically more stable. It was revealed from Figure 13 that the blends retain room temperature after three cycles of applied voltage on and off. This was the great advantage to using this type of blend in practical applications as a self-electrical heater.

However, the growth temperature–time curve can be described by

$$(T - T_m) = (T_m - T_0)(1 - e^{-\tau/t_g}) \qquad (16)$$

where T_m and T_0 are the maximum and room temperature, respectively, and τ_g is the characteristic growth time constant dependent on PE content.

Figure 12(b) shows the evolution of τ_g as a function of PE volume fraction of IIR blend. It is observed that the value of τ_g reached a minimum for PE10 samples and an increase with increasing PE content in the matrix. We concluded that the working power used is absolutely safe, and the growth time is acceptable practically.

Dielectric properties

The dielectric constant (ε) at various temperatures has been estimated, using the formula[1]

$$\varepsilon = Ch/\varepsilon_0 r \qquad (17)$$

where C is the capacitance, h and r are the thickness and the area of the sample, respectively, and ε_0 is the vacuum permittivity (8.854×10^{-12} F/m).

Changes of dielectric constant and tan δ of IIR–PE blends are shown in Figure 14(a). In the case of the PE10 sample, as expected, the marked increases of dielectric constant and tan δ are observed. Again, it is assumed that such an increase is due to the formation of interfacial polarization. For PE10, the increase of dielectric constant and tan δ is due to interface adhesion, which is a higher chance of static energy accumulation and higher polarity. Also, crosslinking density plays an important role in the variation of dielectric constant. Higher CLD results in higher dielectric constant and tan δ. As the PE level becomes higher, the dielectric constant and tan δ decreases. These results indicate that the addition of PE less than 20 wt % has a positive effect in increasing the bonding adhesion in the blend. Therefore, the better mobility transport in the blend medium is believed to induce more efficient interface, leading to higher dielectric constant and tan δ. The variation of dielectric constant with respect to temperature is shown in Figure 14(b). It is observed that the dielectric constant increases linearly with temperature for the PE0, PE10, and PE20 samples, while the dielectric constant increased up to certain temperature and then decreased for PE30 and PE40 samples. The increase of dielectric constant with temperature is due to the formation of dipole segments along the main chains during heating, which increases the value of dielectric constant. With respect to PE30 and PE40 samples, the dielectric constant decreases at a relatively high temperature. This can be explained that at relatively high temperature the number of dipole segments per unit volume is lower due to the dilution of polymer matrix.[1,3,24]

Applicability of blends in EMI shielding effectiveness

To explore the dependence of EMI on the PE content, the changes of EMI characteristics were investigated

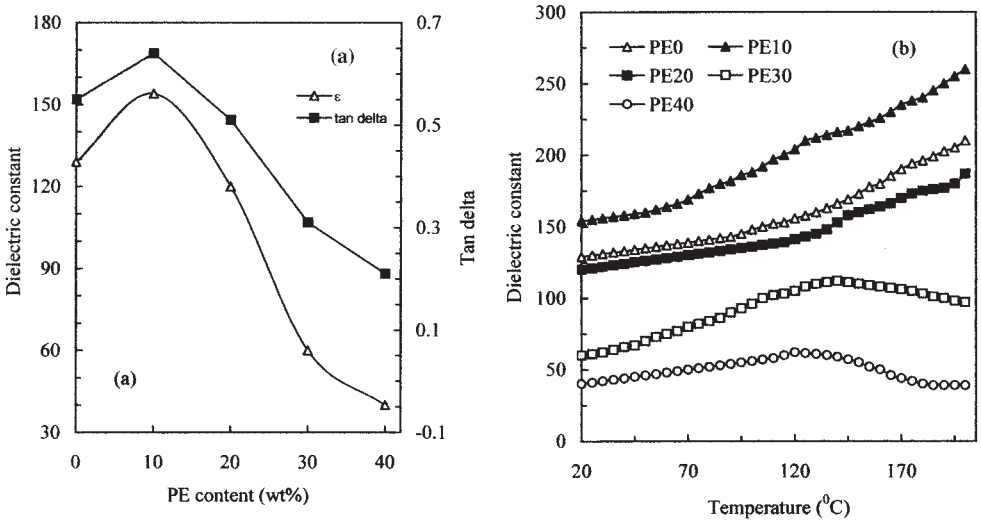

Figure 14 (a) Changes of dielectric constant and tan δ versus PE content in the blend, and (b) the variation of dielectric constant with respect to temperature of IIR–PE blends.

for this system. The EMI offered by a material consists of three different contributions as indicated by the well-known expression[16–18]

$$\text{EMI} = R + A + B \text{ dB} \quad (18)$$

where R is the reflection loss consisting of the reflections from the material boundaries with the surroundings, A is the absorption loss in dB in the material, and B is the successive reflections inside the material, which is negligible in most cases for electrically thick materials.

For conductive blends with a polymer matrix, the EMI is described by

$$\text{EMI} = 10 \log[(1/4\{f_1[f_2 - f_3] + 2(f_1)^{1/2}[f_4 + f_5] + 2[f_2 + f_3]\})] \quad (19)$$

where $f_1 = \sigma/2\omega\varepsilon_0$, $f_2 = \cosh(2d/\delta)$, $f_3 = \cos(2d/\delta)$, $f_4 = \sinh(2d/\delta)$, $f_5 = \sin(2\,d/\delta)$, ω is the angular frequency of the electromagnetic wave, ε_0 is the vacuum dielectric constant, d is the thickness of the material, δ is the skin depth of material, and σ is the DC electrical conductivity.

The effect of PE content on the EMI shielding properties of the IIR blend was investigated. Figure 15(a, b) presents the experimental coefficients of reflection and attenuation of the IIR composites versus PE content. From Figure 15(a), it is noted that the effect of PE content on coefficient of reflection and attenuation of filled and unfilled blends is very high. Clearly, it is noted that the best sample, with 10 wt %, exhibits very high coefficients of reflection and attenuation. When the PE content exceeds 10 wt %, the coefficients of reflection and attenuation of the blend decrease. The increase of PE content above 10 wt % produces no significant modification of the EMI shielding. The increase of coefficients of reflection and attenuation for sample PE0 and PE10 is due to the electromagnetic reflection, which was very high with almost no transmission through the blend. Also, the blend exhibits metallic behavior with the collapse of the electric field component of the electromagnetic radiation occurring when it impinges on the blend material. Hence, it can be concluded that the improvement in coefficients of reflection and attenuation for PE10 sample is attributed to the formation of a conductive mesh and interface adhesion among the CB particles within the IIR–PE blend. Conversely, by increasing PE more than 20 wt %, there is very little interaction of the electromagnetic radiation with the blend, and the transmission of electromagnetic radiation through the blend was high with very little reflection. Figure 15(b, c) presents both the experimental and the theoretical of EMI versus frequency of IIR–PE blends. The theoretical curve corresponding to eq. (19) fits well with the experimental data. Therefore, the proposed blend has an advantage for applications of EMI shielding devices such as radar antenna and microwave.

CONCLUSIONS

During the experiments, the following have been found.

1. The incorporation of PE less than 20 wt % into rubber matrix improves the molecular structure and acts as a compatibilizing agent, whereas the loading of PE more than 20 wt % is useless for improving the network structure of the IIR matrix.

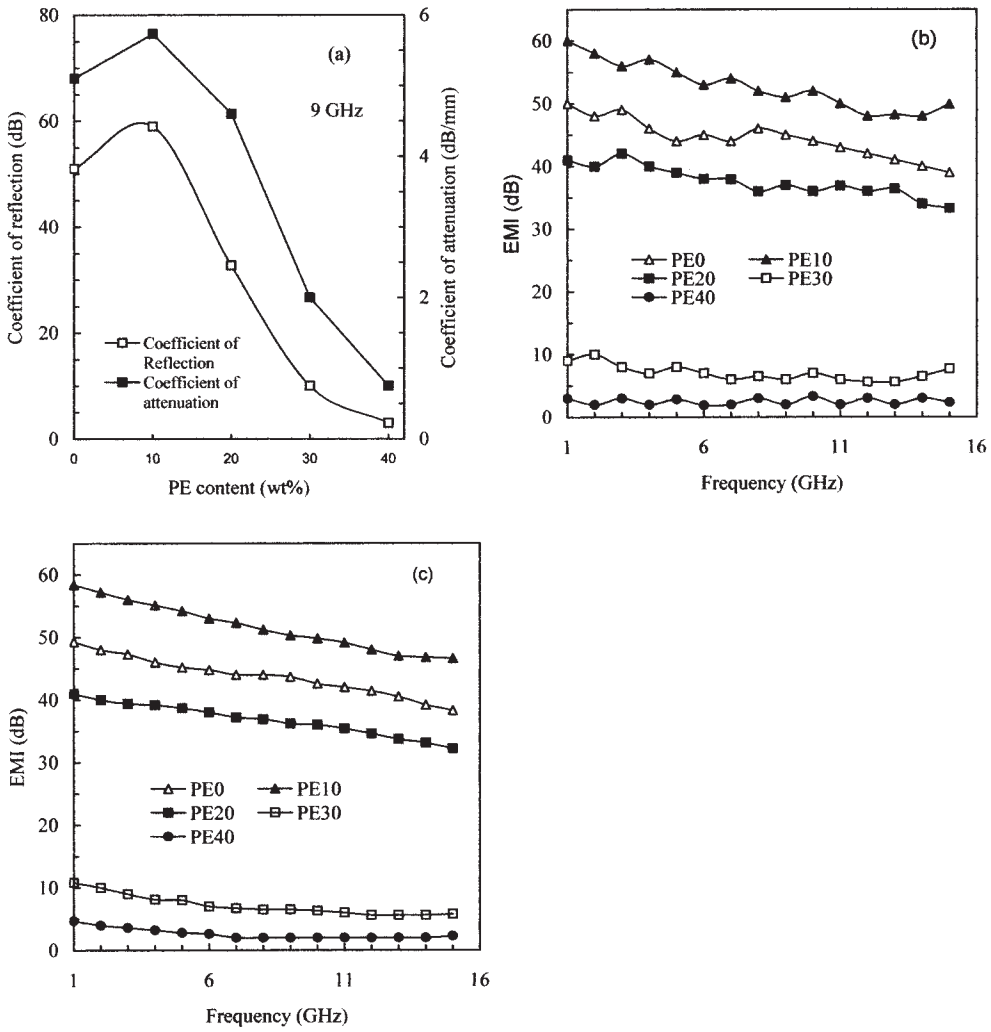

Figure 15 (a) Experimental dependence of coefficients of reflection and attenuation of the IIR composites versus PE content. (b,c) The experimental and theoretical dependence of EMI versus frequency of IIR–PE blend.

2. Room temperature conductivity and mobility carriers of the conducting IIR–PE blend depend on the PE content in the blend. The activation energy of conduction depends on the blend composition. The negative TEP found in this blend revealed that the majority charge carriers are electrons and the Fermi level is pinned by defect states a little above half the gap for PE up to 10 wt % and little below half for PE more than 10 wt %.
3. The *I–V* characteristic of IIR–PE blend shows a current switching.
4. The conductivity decreases linearly with increasing temperature for PE $\leq$ 20 wt %, whereas the conductivity showed a double negative and positive temperature coefficient of conductivity for PE30 and PE40 samples.
5. The ultimate temperature of IIR blends extremely increases in the PE10 sample and returns immediately to initial room temperature when applied power was turned off.
6. The temperature increased linearly with applied field, which makes the proposed blends very useful for temperature sensor applications.
7. The EMI shielding of conductive IIR composites filled with 10 wt % PE is about 61 dB, which gives a better shielding effect. The EMI obtained by measurement approximately corresponds to that obtained by theoretical calculation, so that the EMI shielding of the blends can be predicted in this most frequency used range.

References

1. El-Tantawy, F.; Dishovsky, N.; Dimittrov, N. Polym Testing 2004, 23, 69.
2. El-Tantawy, F.; Dishovsky, N. J Appl Polym Sci 2004, 91, 2756.
3. El-Tantawy, F.; Song, Y. K. Macromol Res 2002, 10, 60.
4. Wootthikanokkhan, J.; Tunjongnawin, P. Polym Testing 2003, 8, 13.
5. Chandrasekhar, P.; Naishaham, K. Synth Met 1999, 105, 115–120.

6. Hussain, M.; Choa, Y. H.; Niihara, K. Composites A 2001, 32, 1689.
7. Philip, J.; Kutty, T. R. N. Mater Chem Phys 2002, 73, 220.
8. Mrooz, O.; Kovalski, A.; Maciak, J. Microelectron Reliability 2001, 41, 773.
9. Dishovsky, N.; Grigorov, M. Mater Res Bull 2000, 35, 403.
10. Sau, K. P.; Chaki, T. K.; Khastgir, D. J Appl Polym Sci 1999, 71, 887.
11. Wang, G.; Li, M.; Chen, X. J Appl Polym Sci 1999, 72, 577.
12. Lee, C. H.; Kim, S. W. J Appl Polym Sci 2000, 78, 2540.
13. Hussain, M.; Choa, Y. H.; Niihara, K. Composites A 2001, 32, 1689.
14. Ismail, H.; Shuhelny, S. S.; Edyham, M. R. Eur Polym J 2002, 38, 39.
15. Marzocca, A. J.; Cerveny, S.; Raimondo, R. B. J Appl Polym Sci 1997, 66, 1092.
16. Yu, G.; Zhang, M. Q.; Zang, H. M. J Appl Polym Sci 1998, 70, 559.
17. Zheng, H.; Zhang, Y.; Peng, Z. Polym Testing 2003, 9, 67.
18. Kaynak, A.; Polcat, A.; Yilmazer, U. Mater Res Bull 1996, 31(10), 1195.
19. Lu, G.; Li, X.; Jiang, H. Compos Sci Technol 1996, 56, 193.
20. Lee, C. Y.; Song, H. G.; Jang, K. S.; Oh, E. J.; Epstein, A. J.; Joo, J. Synth Met 1999, 102, 1346.
21. Xiao-Su, Y.; Song, Y.; Zheng, Q. J Appl Polym Sci 2000, 77, 792.
22. Tao, X.; Pan, Y.; Zheng, Q. J Appl Polym Sci 2001, 79, 2258.
23. L ee, B. O.; Woo, W. J.; Kim, M. S. Macromol Mater Eng 2001, 286, 114.
24. Luo, Y.; Wang, G.; Zhang, B.; Zhang, Z. Eur Polym J 1998, 34, 1221.
25. Srinivas, D.; M. and Reddy, J. Mater Sci Eng 2000, B78, 59.